Computers and Concrete, *Vol. 20, No. 2 (2017) 229-246*
DOI: https://doi.org/10.12989/cac.2017.20.2.229

Dynamic bending response of SWCNT reinforced composite plates subjected to hygro-thermo-mechanical loading

Shivaji G. Chavan* and Achchhe Lal

Department of Mechanical Engineering, S.V.N.I.T, Surat - 395007, India

(Received February 22, 2017, Revised April 4, 2017, Accepted April 7, 2017)

Abstract. The dynamic bending response of single walled carbon nanotube reinforced composite (SWCNTRC) plates subjected to hygro-thermo-mechanical loading are investigated in this paper. The mechanical load is considered as wind pressure for dynamic bending responses of SWCNTRC plate. The dynamic version of the High Order shear deformation Theory (HSDT) for a composite plate with Matrix and SWCNTRC plate is first formulated. Distribution of fibers through the thickness of the SWCNTRC plate could be uniform or functionally graded (FG). The dynamic displacement response is predicted by using Nemarck integration method. The effective material properties of SWCNTRC are estimated by using micromechanics based modeling approach. The effect of different environmental condition, volume fraction of SWCNT, Width-to-thickness ratio, wind pressure, different SWCNTRC-FG plates, boundary condition, E1/E2 ratio, different temperature on dynamic displacement response is investigated. The dynamic displacement response is compared with the available literature and it shows good agreement.

Keywords: dynamic analysis; SWCNTRC-FG plate; HSDT; hygro-thermo-mechanical load; micromechanics; newmark integration method

1. Introduction

The single walled carbon nanotube reinforced composite (SWCNTRC) broadly applied in the field of mechanical, civil, aerospace industries, missile, automobile and any other industries. They are subjected to environmental condition during service life. They operate in a verity of thermal and moisture environments. These hygro-thermal effects are results of temperature and moisture content variation and are the different in the thermal and hygro properties of the composites. In the available literature much of the published works on dynamic response of composite structure as follows. Kumar *et al*. (2003) reported the dynamic instability characteristics of laminated composite plates subjected to partial follower edge load with damping. Liew *et al*. (2004) investigated dynamic analysis of laminated composite plates with piezoelectric sensor/actuator patches using the FSDT mesh-free method. Chen *et al*. (2005) developed State-space approach for statics and dynamics of angle-ply laminated cylindrical panels in cylindrical bending. Agbossou *et al*. (2006) presented a layered approach to the non-linear static and dynamic analysis of rectangular reinforced concrete slabs. Liew *et al.* (2007) presented dynamic stability analysis of composite laminated cylindrical panels via the mesh-free kp-Ritz method. Patel *et al*. (2007) investigated dynamic instability analysis of stiffened shell panels subjected to partial edge loading along the edge. They used eight-noded isoperimetric degenerated shell element and a compatible three-noded curved beam element to model the shell panels and the stiffeners, respectively. Santiuste *et al.* (2008) presented dynamic analysis of bending–torsion coupled composite beams using the Flexibility Influence Function Method. Girhammar *et al*. (2009) presented exact dynamic analysis of composite beams with partial interaction. They also studied partial differential equations and general solutions for the deflection and internal actions and the pertaining consistent boundary conditions for composite Euler–Bernoulli members with interlayer slip subjected to general dynamic loading. Lei *et al.* (2015) studied elastic-dynamic analysis of carbon nanotube-reinforced functionally graded plates. The dynamic instability of damped composite skew plates under non-uniform in-plane periodic loading was investigated by Kumar *et al.* (2015). Shao *et al.* (2016) presented transient response analysis of cross-ply composite laminated rectangular plates with general boundary restraints by the method of reverberation ray matrix. Li *et al.* (2016) performed a dynamic analysis approach for identifying the elastic properties of unstitched and stitched composite plates. Salami *et al*. (2016) developed dynamic extended high order sandwich panel theory for transient response of sandwich beams with carbon nanotube reinforced face sheets. The nonlinear dynamic response of nanotube-reinforced composite plates resting on elastic foundations in thermal environments was studied by Wang *et al.* (2012). Zhang *et al.* (2013) performed on nonlinear dynamics analysis of a deploying composite laminated cantilever plate by using FEM. Mechanical strength of self–compacting mortar containing nanoparticles using wavelet–based support vector machine the mathematical modeling was developed by Khatibinia *et*

*Corresponding author, Ph.D.
E-mail: shivajigchavan@gmail.com

http://www.techno-press.org/?journal=cac&subpage=8
ISSN: 1598-8198 (Print), 1598-818X (Online)

al. (2016). Shariq *et al.* (2017) studied effect of the experimental investigation of effect on time dependent deflection of reinforced beam due to creep and shrinkage.

Asadi *et al.* (2014) investigated nonlinear free vibration and primary/secondary resonance analyses of shape memory alloy (SMA) fiber reinforced hybrid composite beams with symmetric and asymmetric lay-up. The modeling and active shape/stress control of laminated beams subjected to the static loading with integrated/embedded shape memory alloy (SMA) layer were studied by Bodaghi *et al*. (2013). Ebrahimi and Habibi (2017) presented nonlinear eccentric low-velocity impact response of polymer-CNT-fiber multiscale nano-composite plate on elastic foundations in hydrothermal conditions using the finite element method. Considering the agglomeration effect of single-walled carbon nanotubes, free vibration characteristics of functionally graded (FG) Nano composite sandwich beams resting on Pasternak foundation were studied by Kamarian *et al*. (2015). Kamarian *et al*. (2016) investigated the natural frequency analysis of non-uniform nanocomposite beams with surfacebonded piezoelectric layers by considering the agglomeration effect of Carbon Nanotubes (CNTs). They also predicted material properties of the nanocomposite beam employing Eshelby-Mori-Tanaka approach based on an equivalent fiber and compared with available experimental data in the literature.

Zidi *et al.* (2014) studied the bending response of functionally graded material (FGM) plate resting on elastic foundation and subjected to hygro-thermo-mechanical loading. Al-Basyouni *et al.* (2015) studied bending and dynamic behaviors of functionally graded (FG) micro beam formulation and a modified couple stress theory (MCST) that considers a variable length scale parameter in conjunction with the neutral axis concept. Benguediab *et al*. (2014) investigated the mechanical buckling properties of a zigzag double-walled carbon nanotube (DWCNT) with both chirality and small scale effects. Belabed *et al*. (2016) presented an efficient and simple higher order shear and normal deformation theory for functionally graded material (FGM) plates. Tounsi *et al.* (2016) presented a new 3-unknown non-polynomial shear deformation theory for the buckling and vibration analyses of functionally graded material (FGM) sandwich plates. Houari *et al*. (2016) developed a new simple higher-order shear deformation theory for bending and free vibration analysis of functionally graded (FG) plates. Tounsi *et al.* (2013) presented the thermo-elastic bending analysis of functionally graded sandwich plates for transverse shear deformation effects by using refined trigonometric shear deformation theory (RTSDT). Bellifa *et al.* (2015) developed a new first-order shear deformation theory for bending and dynamic behaviors of functionally graded plates. Bennoun *et al.* (2014) developed a new five variable refined plate theory for the free vibration analysis of functionally graded sandwich plates.

The new trigonometric higher-order theory including the stretching effect for the static analysis of advanced composite plates such as functionally graded plates was developed by Bousahla *et al.* (2013). Hebali *et al*. (2014) developed a new quasi-three-dimensional (3D) hyperbolic shear deformation theory for the bending and free vibration analysis of functionally graded plates. Mahi *et al*. (2013) presented a new hyperbolic shear deformation theory applicable to bending and free vibration analysis of isotropic, functionally graded, sandwich and laminated composite plates. Mezian *et al.* (2015) investigated an efficient and simple refined shear deformation for the vibration and buckling of exponentially graded material sandwich plate resting on elastic foundations under various boundary conditions. Hamidi *et al.* (2015) studied a simple but accurate sinusoidal plate theory for the thermo-mechanical bending analysis of functionally graded sandwich plates. Laboratory *et al.* (2015) developed a simple and refined trigonometric higher-order beam theory for bending and vibration of functionally graded beams. A zero-order shear deformation theory for free vibration analysis of functionally graded (FG) nanoscale plates resting on elastic foundation presented by Bounouara *et al.* (2016). Yahia *et al*. (2015) developed wave propagation in functionally graded plates with porosities using various higher-order shear deformation plate theories. Laboratory *et al.* (2015) developed theory for higher-order variation of transverse shear strain through the depth of the Nano beam, and satisfy the stress-free boundary conditions on the top and bottom surfaces of the nanobeam. Bourada *et al*. (2016) presented Buckling analysis of isotropic and orthotropic plates using a novel four variable refined plate theory.

Benahmed *et al*. (2017) developed an efficient and simple quasi-3D hyperbolic shear deformation theory for bending and vibration analyses of functionally graded (FG) plates resting on two-parameter elastic foundation. Beldjelili *et al.* (2016) discussed the hygro-thermo-mechanical bending behavior of sigmoid functionally graded material (S-FGM) plate resting on variable two-parameter elastic foundations using a four-variable refined plate theory. Bouderba *et al.* (2106) developed and validated a simple first-order shear deformation theory for a variety of numerical examples of the thermal buckling response of functionally graded sandwich plates with various boundary conditions. Chikh *et al.* (2017) presented a simplified higher order shear deformation theory (HSDT) for thermal buckling analysis of cross-ply laminated composite plates. Bouafia *et al.* (2017) investigated size dependent bending and free flexural vibration behaviors of functionally graded (FG) nanobeams using a nonlocal quasi-3D theory in which both shear deformation and thickness stretching effects. Bending and buckling analyses of functionally graded material (FGM) size-dependent nanoscale beams including the thickness stretching effect were addressed by Larbi *et al*. (2015). Bounouara *et al.* (2016) presented a new nonlocal hyperbolic refined plate model for free vibration properties of functionally graded (FG) plates. Ahouel *et al.* (2016) developed a nonlocal trigonometric shear deformation beam theory based on neutral surface position for bending, buckling, and vibration of functionally graded (FG) Nano beams using the nonlocal differential constitutive relations of eringen. Tagrara *et al.* (2015) developed a trigonometric refined beam theory for the bending, buckling and free vibration analysis of carbon

nanotube-reinforced composite (CNTRC) beams resting on elastic foundation.

The literature review presented above shows that most of the researchers has developed different plate theories for investigate the bending, buckling and vibration characteristics of composite structure subjected to mechanical and hygro-thermo-mechanical loading. Earlier authors' are investigated of bending, vibration and post buckling of liner-nonlinear laminated and functionally graded SWCNT, carbon or glass fiber polymer composite structure subjected to hygro-thermo-mechanical loading. No work dealing with dynamic bending response of SWCNT reinforced composite plates subjected to hygro-thermo-mechanical loading is reported in the literature to the best of the authors' knowledge. The contribution of this paper is to investigate the dynamic bending response of SWCNT response of SWCNT functionally graded reinforced Composites Plate subjected to hygro-thermo-mechanical loading based on HSDT frame work.

The main objective of this study to extend the Seven degree of freedom of Finite element formulation based on HSDT to the dynamic bending response of SWCNTRC-FG plates subjected to hygro-thermo-mechanical loading, Motivated by aircraft wing structure under hygro-thermal environmental condition and wind pressure as mechanical loading. In polymer Nano-composite material is mead up Matrix and SWCNT. The matrix material is more sensitive in hygro-thermal environment (combine temperature and moisture). Mechanical load is considered as wind pressure; the wind pressure is applied on composite structure with hygro-thermal uniform filed. In present study, an attempted is mead to investigate above mention problem using Newmark's time integration method based on HSDT. The properties of SWCNTRC plate is estimated by using micromechanics approach. The main objective of this work is too focused on dynamic bending response subjected to different environmental and loading condition of composite structure. The results obtained for dynamic displacement response for SWCNTRC plate with width-to-thickness ratio, boundary condition, wind pressure, different FG plate, E_1/E_2 ratio and volume fraction of SWCNT.

2. Seven degree of finite element formulation

In the present work, finite element formulation for SWCNTRC plate is based on HSDT because it represents the kinematics better, not require shear correction factors, and can yield more accurate stress distributions (Reddy 1982).

2.1 The displacement field

Displacement field is taken from (Chavan *et al.* 2017)

$$\bar{u} = u + z\psi_x - z^3\frac{4}{3h^2}\left(\frac{\partial w}{\partial x} + \psi_x\right) = u + f_1(z)\psi_x + f_2(z)\frac{\partial w}{\partial x}$$
$$\bar{v} = v + z\psi_y - z^3\frac{4}{3h^2}\left(\frac{\partial w}{\partial y} + \psi_y\right) = u + f_1(z)\psi_y + f_2(z)\frac{\partial w}{\partial y} \quad (1)$$
$$\bar{w} = w$$

Where, $f_1(z) = C_1 z - C_2 z^3$, and $f_2(z) = -C_4 z^3$; $C_1 = 1, C_4 = C_2 = \frac{4}{3h^2}$;

From Eq. (1), it is seen that the expressions for in-plane displacement $\bar{u}$ and $\bar{v}$ involve the derivatives of out of plane displacement w. As a result of this, second order derivatives would be present in the strain vector, thus necessitating the employment of C^1 continuity for finite element analysis. The complexity and difficulty involved with making a choice of C^1 continuity are well known.

Expressing the displacement field in the following form avoids this

$$\bar{u} = u + f_1(z)\psi_x + f_2(z)\theta_x = u + f_1(z)\psi_1 + f_2(z)\theta_1$$
$$\bar{v} = v + f_1(z)\psi_y + f_2(z)\theta_y = u + f_1(z)\psi_2 + f_2(z)\theta_2 \quad (2)$$
$$\bar{w} = w$$

Where

$$\frac{\partial w}{\partial x} = \theta_x = \theta_1 ; \frac{\partial w}{\partial y} = \theta_y = \theta_2$$

It can be seen that the number of degrees of freedom (DOF) per node, by treating θ_x and θ_y as separate DOFs, increases from 5 to 7 for HSDT model. However, the strain vector will be having only first order derivatives, and hence a C^0 continuous element would be sufficient for the finite element analysis, (Chavan *et al*. 2017). In the present study, nine noded quadratic isoperimetric elements have been used with 63 DOF per element, as shown in Fig. 2.

2.2 Strain displacement relation

The SWCNTRC plate of present's dynamic bending response, linear mechanical strain vector strain vector $\{\varepsilon_M\}$ due to mechanical load and hygro-thermal strain vectors $\{\varepsilon_{hyro}\}$ corresponding to displacement fields are

$$\{\varepsilon\} = \{\varepsilon_M\} + \{\varepsilon_{hyro}\} \quad (3)$$

Strain vector $\{\varepsilon_M\}$ due to Wind pressure (mechanical loading) only, can be written as

$$\{\varepsilon_M\} = \{\varepsilon_x\ \varepsilon_y\ \gamma_{xy}\ \gamma_{xz4}\ \gamma_{yz}\ \}^T \quad (4)$$

Where, $\varepsilon_i^0 (i = 1, 2 \ldots 6)$ and $k_i^0 (i = 1, 2 \ldots 6)$ are mid-plane strains and curvatures and are given by, (Chavan *et al*. 2017)

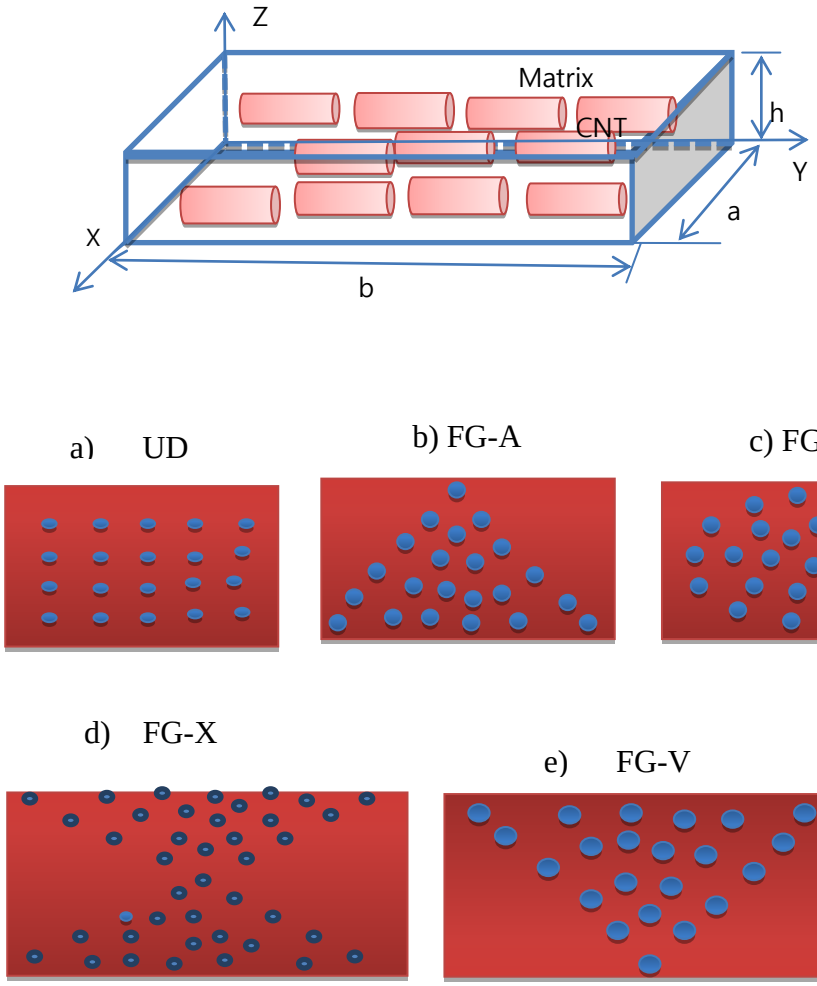

Fig. 1 SWCNTRC plate and Different configuration of SWCNT-FG (a)UD, (b) FG-A, (c)FG-O, (d) FG-X and (e) FG-V

$$\varepsilon_x = \varepsilon_1^o + z(\mathrm{k}_1^o + \mathrm{z}^2\mathrm{k}_1^2)$$

$$\varepsilon_y = \varepsilon_2^o + z(\mathrm{k}_2^o + \mathrm{z}^2\mathrm{k}_2^2)$$

$$\varepsilon_3 = 0\,,\ \gamma_{xy} = \varepsilon_4^o + \mathrm{z}^2\mathrm{k}_4^2 \qquad (5)$$

$$\gamma_{xz} = \varepsilon_5^o + \mathrm{z}^2\mathrm{k}_5^2$$

$$\gamma_{yz} = \varepsilon_6^o + z(\mathrm{k}_6^o + \mathrm{z}^2\mathrm{k}_6^2)$$

Where

$$\varepsilon_1^o = \frac{\partial u}{\partial x}, \mathrm{k}_1^o = \frac{\partial \psi_x}{\partial x}, \mathrm{k}_1^2 = -\frac{4}{3h^2}\left(\frac{\partial^2 w}{\partial x^2} + \frac{\partial \psi_x}{\partial x}\right)$$

$$\varepsilon_2^o = \frac{\partial u}{\partial y}, \mathrm{k}_2^o = \frac{\partial \psi_y}{\partial y}, \mathrm{k}_2^2 = -\frac{4}{3h^2}\left(\frac{\partial^2 w}{\partial y^2} + \frac{\partial \psi_y}{\partial y}\right)$$

$$\varepsilon_6^o = \frac{\partial u}{\partial x} + \frac{\partial v}{\partial y}, \mathrm{k}_6^o = \frac{\partial \psi_x}{\partial y} + \frac{\partial \psi_y}{\partial x}, \mathrm{k}_6^2 = -\frac{4}{3h^2}\left(\frac{\partial \psi_x}{\partial y} + \frac{\partial \psi_y}{\partial x} + 2\frac{\partial^2 w}{\partial xy}\right)$$

$$\varepsilon_4^o = \psi_y + \frac{\partial w}{\partial y}, \mathrm{k}_4^2 = -\frac{4}{h^2}\left(\psi_y + \frac{\partial w}{\partial y}\right)$$

$$\varepsilon_5^o = \psi_x + \frac{\partial w}{\partial x}, \mathrm{k}_5^2 = -\frac{4}{h^2}\left(\psi_x + \frac{\partial w}{\partial x}\right)$$

Here, the mid-plane strain vector can be written as

$$\left\{\bar{\varepsilon}\right\} = \left(\varepsilon_1^0 \ \ \varepsilon_2^0 \ \ \varepsilon_6^0 \ \ k_1^0 \ \ k_2^0 \ \ k_6^0 \ \ k_1^2 \ \ k_2^2 \ \ k_6^2 \ \ \varepsilon_4^0 \ \ \varepsilon_5^0 \ \ k_4^2 \ \ k_5^2\right), \quad (6)$$

The vector $\left\{\varepsilon_{hyro}\right\}$ due to hygro-thermal loading can be written as

$$\left\{\varepsilon_{hyro}\right\} = \Delta T\left\{\alpha_x \alpha_y \alpha_{xy} 00\right\}^T + \Delta C\left\{\chi_x \chi_y \chi_{xy} 00\right\}^T \qquad (7)$$

2.3 Constitutive equation (stress-strain relation)

Stress-strain relation for SWCNTRC plate due to hygro-thermo-mechanical loading is given by

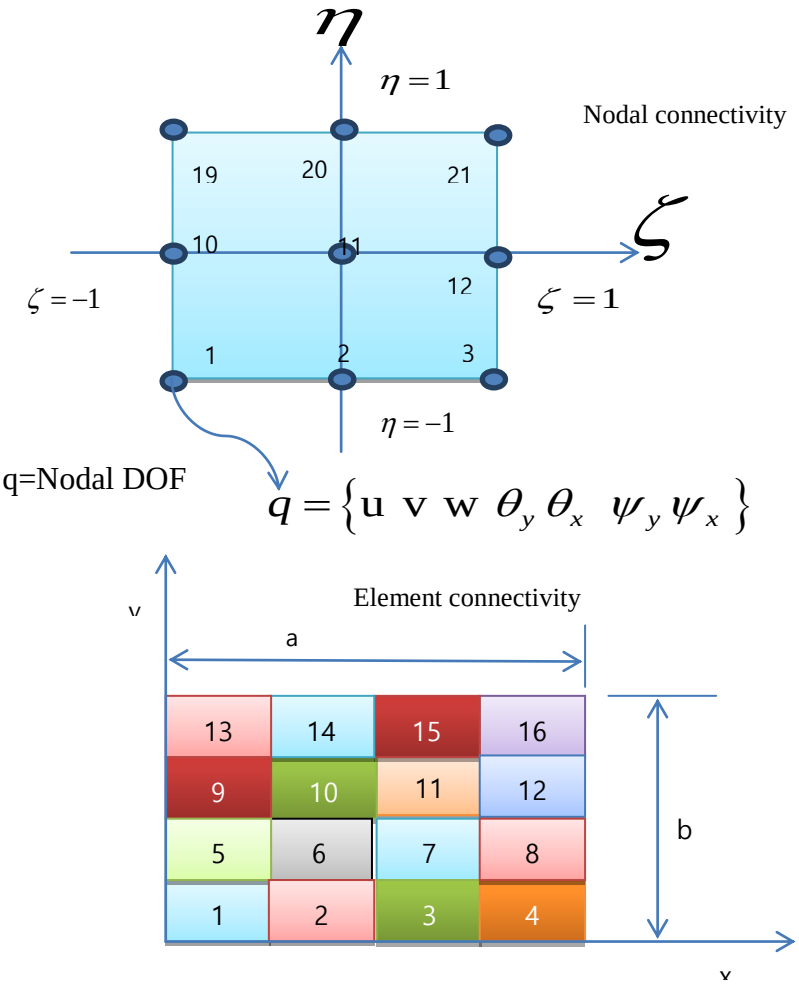

Fig. 2 SWCNTRC plate meshed with 4X4 using nine noded isoperimetric element

$$\begin{Bmatrix}\sigma_x\\ \sigma_y\\ \tau_{xy}\\ \tau_{yz}\\ \tau_{xz}\end{Bmatrix}=\begin{bmatrix}\bar{Q}_{11} & \bar{Q}_{12} & \bar{Q}_{16} & 0 & 0\\ \bar{Q}_{12} & \bar{Q}_{22} & \bar{Q}_{26} & 0 & 0\\ \bar{Q}_{16} & \bar{Q}_{26} & \bar{Q}_{66} & 0 & 0\\ 0 & 0 & 0 & \bar{Q}_{44} & \bar{Q}_{45}\\ 0 & 0 & 0 & \bar{Q}_{45} & \bar{Q}_{55}\end{bmatrix}\begin{Bmatrix}\varepsilon_x-\alpha_x\Delta T-\chi_x\Delta C\\ \varepsilon_y-\alpha_y\Delta T-\chi_y\Delta C\\ \gamma_{xy}-\alpha_{xy}\Delta T-\chi_{xy}\Delta C\\ \gamma_{yz}\\ \gamma_{xz}\end{Bmatrix} \quad (8)$$

The hygro-thermal coefficient in (x, y) coordinate is given by

$$\begin{Bmatrix}\alpha_x & \chi_x\\ \alpha_y & \chi_y\\ \alpha_{xy} & \chi_{xy}\end{Bmatrix}=\begin{Bmatrix}\sin^2\theta & \cos^2\theta\\ \cos^2\theta & \sin^2\theta\\ 2\sin\theta\cos\theta & -2\sin\theta\cos\theta\end{Bmatrix}\begin{Bmatrix}\alpha_{11} & \chi_{11}\\ \alpha_{22} & \chi_{22}\end{Bmatrix} \quad (9)$$

Where, α and χ is the coefficients of thermal expansion and coefficients of hygral expansion respectively.

2.4 Micromechanics analysis

The effective material properties of SWCNTRC plate are obtained by using micromechanics. The carbon nanotube composite plate is mead up of matrix PMMA and SWCNT. The bounding of SWCNT and matrix is taken to be perfect. In this study consider the SWCNTRC plate with five configurations of SWCNTRC-FG plates over the thickness as shown in Fig 1. The mathematically model of SWCNTRC-FG plates is given by (Chavan 2017).

$$V_{CNT}=V^* \quad \text{----------UD}$$

$$V_{CNT}=2\left(1-\frac{2|z|}{h}\right)V^* \quad \text{-------FG-O}$$

$$V_{CNT}=\left(\frac{2|z|+h}{h}+\right)V^* \quad \text{------FG-V}$$

$$V_{CNT}=4\left(\frac{|z|}{h}+\right)V^* \quad \text{----------FG-X} \quad (10)$$

$$V_{CNT}=4\left(1-\frac{2|z|}{h}\right)V^* \text{--------FG-}A$$

$$V^*=\frac{W_{CNT}}{W_{CNT}+\left(\frac{\rho_{CNT}}{\rho_m}\right)(1-W_{CNT})}$$

Where, W_{CNT}, and ρ_{CNT} are mass fraction and density of SWCNT respectively. ρ_m is density of matrix.

Mass density and total volume fraction of SWCNTRC is defined as

$$\rho = V_{CNT}\rho_{CNT} + V_m\rho_m \text{ and } V^{CNT} + V^m = 1 \tag{11}$$

The matrix material is more sensitive to the temperature and moisture, the hygro-thermal degradation of matrix property only considered for evaluating SWCNTRC material properties. The mechanical property retention ratio is given by Gadade *et al.* (2016)

$$Fm = \left[\frac{T_{CW} - T}{T_{C0} - T_0}\right] \tag{12}$$

Where, $T = T_0 + \Delta T$ is the temperature at which change the property of composite material. T_{CW} and T_{CO} are fiber transition temperature for wet and reference dry condition respectively. The fiber transition temperature can be defined as Gadade *et al*. (2016)

$$T_{CW} = \left(0.005C^2 - 0.1C + 1.0\right)T_{C0} \tag{13}$$

Where, $C = C_0 + \Delta C$ is the weight percentage of moisture in the matrix material.

Elastic Properties of SWCNTRC plate are defined by (Gadade *et al.* 2016)

$$E_{11} = E_{11}^{CNT}V^{CNT} + FmE_mV_m \tag{14}$$

$$E_{22} = \left(1 - \sqrt{V^{CNT}}\right)FmE_m + \frac{FmE_m\sqrt{V^{CNT}}}{1 - \sqrt{V^{CNT}}\left(1 - \frac{FmE_m}{E_{22}^{CNT}}\right)} \tag{15}$$

$$G_{12} = \left(1 - \sqrt{V^{CNT}}\right)FmG_m + \frac{FmG_m\sqrt{V^{CNT}}}{1 - \sqrt{V^{CNT}}\left(1 - \frac{FmG_m}{E_{22}^{CNT}}\right)} \tag{16}$$

$$v_{22} = v_{12}^{CNT}V^{CNT} + v_mV_m \tag{17}$$

$$\alpha_{11} = \frac{\alpha^{CNT}V^{CNT}E_{11}^{CNT} + \alpha^mV^mE^m}{V^{CNT}E_{11}^{CNT} + V^mE^m} \tag{18}$$

$$\alpha_{22} = \left(1 + v^{CNT}\right)\alpha^{CNT}V^{CNT} + \left(1 + v^m\right)\alpha^mV^m - v^m\alpha_{11} \tag{19}$$

$$\chi_{11} = \frac{\chi^{CNT}V^{CNT}E_{11}^{CNT}C_{CNTm} + \chi^mV^mE_{11}^m}{E_{11}^{CNT}\left(V^{CNT}\rho^{CNT}C_{CNTm} + V^m\rho^m\right)}\rho \tag{20}$$

$$\chi_{22} = \frac{V^{CNT}\left(1 + v^{CNT}\right)C_{CNTm}\chi^{CNT} + V^m\left(1 + v^m\right)\chi^m}{\left(V^{CNT}\rho^{CNT}C_{CNTm} + V^m\chi^m\right)}\rho - v_{12}^{CNT}\chi_{11} \tag{21}$$

C_{CNTm} is the moisture concentration ratio. χ^{CNT} and χ^m are the swelling coefficient of the CNT and matrix respectively, $\chi^{CNT} = 0$.

2.5 Potential energy of SWCNTRC plate

The total strain energy of SWCNTRC plate is consist of strain energy due to wind pressure and strain energy due to hydrothermal loading is defined as

$$U = U_1 + U_2 \tag{22}$$

Strain energy due to wind pressure (mechanical loading) of SWCNTRC plate is defined as

$$U_1 = \frac{1}{2}\int_A \{\varepsilon_M\}^T [\sigma]\, dA \tag{23}$$

The strain energy due to hygro-thermal (combined temperature and moisture) loading is given by

$$U_2 = \frac{1}{2}\int_A \left[N_{THx}\right]\left(\frac{\partial u}{\partial x}\right)^2 + \left[N_{THy}\right]\left(\frac{\partial v}{\partial x}\right)^2 + 2\left[N_{THxy}\right]\left(\frac{\partial u}{\partial x}\right)^2\left(\frac{\partial v}{\partial x}\right)^2 dA \tag{24}$$

$$U_2 = \frac{1}{2}\int_A \begin{Bmatrix}\left(\frac{\partial u}{\partial x}\right)\\ \left(\frac{\partial v}{\partial x}\right)\end{Bmatrix}^T \begin{bmatrix} N_{THx} & N_{THxy}\\ N_{THxy} & N_{THy}\end{bmatrix} \begin{Bmatrix}\left(\frac{\partial u}{\partial x}\right)\\ \left(\frac{\partial v}{\partial x}\right)\end{Bmatrix} dA \tag{25}$$

Where, N_{THx}, N_{THy} and N_{THxy} are the hygro-thermal stress resultants.

2.6 kinetic energy of SWCNTRC plate

The kinetic energy of the SWCNTRC plate is given by

$$T = \frac{1}{2}\iint\left[\sum_{k=1}^{N}\int_{h_k}^{h_{k+1}} \rho_k \left\{\dot{u}_k\dot{v}_k\dot{w}_k\right\}\left\{\dot{u}_k\dot{v}_k\dot{w}_k\right\}^T dz\right]dxdy \tag{26}$$

Where, ρ_k is mass density and $\dot{u}_k\dot{v}_k\dot{w}_k$ are velocity along x,y and z direction.

2.7 finite element modeling

The finite element method (FEM) is a numerical technique being used for finding an approximate solution to

a wide variety of engineering problems through bending Approach. In the present paper nine nodded isoperimetric elements with seven degree of freedom per node is employed for finite element plate modeling.

$$q=\sum_{i=1}^{NN}N_i q_i;\qquad x=\sum_{i=1}^{NN}N_i x_i\ ;\ \ y=\sum_{i=1}^{NN}N_i y_i \tag{27}$$

Shape function of isoperimetric nine noded elements is taken from (Reddy 2000) as shown in Fig. 2.

$$\begin{aligned}
N_1&=\frac{1}{4}\left(\zeta^2-\zeta\right)\left(\eta^2-\eta\right)\\
N_2&=\frac{1}{4}\left(\zeta^2+\zeta\right)\left(\eta^2-\eta\right)\\
N_3&=\frac{1}{4}\left(\zeta^2+\zeta\right)\left(\eta^2+\eta\right)\\
N_4&=\frac{1}{4}\left(\zeta^2-\zeta\right)\left(\eta^2+\eta\right)\\
N_5&=\frac{1}{2}\left(1-\zeta^2\right)\left(\eta^2+\eta\right)\\
N_6&=\frac{1}{2}\left(\zeta^2+\zeta\right)\left(1-\eta^2\right)\\
N_7&=\frac{1}{2}\left(1-\zeta^2\right)\left(\eta^2+\eta\right)\\
N_8=\frac{1}{2}\left(\zeta^2-\zeta\right)\left(1-\eta^2\right);\ &N_9=\left(1-\zeta^2\right)\left(1-\eta^2\right)
\end{aligned}\tag{28}$$

Where, N_i and q_i are the interpolation function and vector of unknown displacements for the i^{th} node, respectively, NN is the number of nodes per element and x_i and y_i are Cartesian coordinate of the i^{th} node. The equilibrium Equation governing the present problem for the SWCNTRC plate can obtain by minimizing potential energy with respect to displacement, can be written as

$$\frac{\partial U}{\partial q}=0 \tag{29}$$

Substitute Eq. (25) and Eq. (23) into Eq. (22) again substitute Eq. (22) into Eq. (29) we get

$$\left\{F_i\right\}=[\mathrm{K}_{ij}]\left\{q_i\right\} \tag{30}$$

$$\left\{q\right\}=\left\{F\right\}\left[K\right]^{-1} \tag{31}$$

Where, $\left\{F_i\right\}=\sum_{e=1}^{NE}\left\{F_M\right\}^e+\sum_{e=1}^{NE}\left\{F_{TH}\right\}^e$ is global force vector (mechanical and hygro-thermal loading), $\left[K_{ji}\right]=\sum_{e=1}^{NE}\left[K_{ij}^e\right]$ is global stiffness matrix, $\left\{q_i\right\}=\sum_{e=1}^{NE}\left\{q\right\}^e$ is global displacement vector.

Eq. (31) is then solved for SWCNTRC plate acted upon by hygro-thermo-mechanical loading to obtained displacement.

3. Governing equation

The governing equation for the dynamic response of SWCNTRC plate can be derived using Hamilton principle, which is generalization of the virtual displacement. Lagrange equation for a conservative system can be written as

$$\frac{d}{dt}\left(\frac{\partial T}{\partial\left\{\dot{q}_i\right\}}\right)+\frac{\partial U}{\partial\left\{q_i\right\}}+\frac{\partial}{\partial\left\{q_i\right\}}\left\{\frac{1}{2}\int_V\left\{q\right\}^2 dv\right\}=0 \tag{32}$$

Substitute U and T from Eqs. (22) and (26) and Eq. (31) into Eq. (32) one obtained as

$$\left[M\right]\left\{\ddot{q}\right\}+\left[K\right]\left\{q\right\}=\left\{F\right\} \tag{33}$$

Where, [M]=mass matrix, $\left\{\ddot{q}\right\}$ =acceleration vector, $\left\{\dot{q}\right\}$ =velocity vector and $\left\{q\right\}$ is displacement vector.The Numerical time integration by newmark method (Reddy 2000) as

$$\left\{q\left(t_{s+1}\right)\right\}=\left\{q\left(t_s\right)\right\}+\delta t_s\left\{\dot{q}\left(t_s\right)\right\}+\frac{1}{2}\left(\delta t_s\right)^2\left\{\ddot{q}\left(t_{s+\gamma}\right)\right\} \tag{34}$$

$$\left\{\dot{q}\left(t_{s+1}\right)\right\}=\left\{\dot{q}\left(t_s\right)\right\}+\delta t_s\left\{\ddot{q}\left(t_{s+\alpha}\right)\right\} \tag{35}$$

$$\left\{\ddot{q}\left(t_{s+\alpha}\right)\right\}=\left(1+\alpha\right)\left\{\ddot{q}\left(t_s\right)\right\}+\alpha\left\{\ddot{q}\left(t_{s+1}\right)\right\},\quad 0\le\alpha\le 1 \tag{36}$$

$\delta t_s=t_{s+1}-t_s$, δt_s is time increment and t_s is $\delta t=0.02$ current time and t_{s+1} is next time. Substituting the Eq. (36) into the Eq. (34) and solving $\left\{\ddot{q}\right\}$, We obtained.

$$\left\{\dot{q}\right\}_{s+1}=\left\{\dot{q}\right\}_s+a_1\left\{\ddot{q}\right\}_s+a_2\left\{\ddot{q}\right\}_{s+1} \tag{37}$$

$$\left\{\ddot{q}\right\}_{s+1}=a_3\left(\left\{q\right\}_{s+1}-\left\{q\right\}_s\right)-a_4\left\{\dot{q}\right\}_s-a_5\left\{\ddot{q}\right\}_s \tag{38}$$

Where,

$a_1=\left(1-\alpha\right)\delta t_s,\ a_2=\alpha\delta t_s,\ a_3=\frac{2}{\gamma\left(\delta t_s\right)^2},a_4=a_3\delta t_s,a_5=\frac{\left(1-\gamma\right)}{\gamma}$

$\gamma\ge\alpha\ge\frac{1}{2}$ Unconditional stable.

$\gamma<\alpha,\alpha\ge 0.5$ Conditional stable.

Table 1 Temperature dependent material property of (10, 10) SWCNT is given by (Wang *et al*. 2012) (L=9.23 nm, R=0.68, t=0.067, $v_{12}^{CNT}=0.172$, $\rho^{CNT}=1400kg/m^3$)

Temperature(K)	E_{11}^{CNT} (TPa)	E_{22}^{CNT} (TPa)	G_{12}^{CNT} (TPa)	$\alpha_{11}^{CNT}(\times10^{-6}/\mathrm{K})$	$\alpha_{22}^{CNT}(\times10^{-6}/\mathrm{K})$
300	5.6466	7.0800	1.9445	3.4584	5.1682
500	5.5308	6.9348	1.9643	4.5361	5.0189
700	5.4744	6.8641	1.9644	4.6677	4.8943

The second equation in Eq. (37) with $[M]_{s+1}$ and using Eq. (40) at $t=t_{s+1}$ to replace, $[M]_{s+1}\{\ddot{q}\}_{s+1}$ we obtained

$$\left[\hat{\bar{K}}\right]\{\ddot{q}\}_{s+1}=\{\hat{\bar{F}}\} \tag{39}$$

Where, $\left[\hat{K}\right]=[K]_{s+1}+a_3[M]_{s+1}$,

$\left[\hat{F}\right]=[F]_{s+1}+[M]_{s+1}\left(a_3\{q\}_s+a_4\{\dot{q}\}_s+a_5\{\ddot{q}\}_s\right)$

An alternative from of Eq. (38) is given by

$$\left[\hat{\bar{K}}\right]\{\ddot{q}\}_{s+1}=\left\{\hat{\bar{F}}\right\} \tag{40}$$

Where, $\left[\hat{\bar{K}}\right]=[M]_{s+1}+\frac{1}{a_3}[K]_{s+1}$;

$\left[\hat{\bar{F}}\right]=[F]_{s+1}-[K]_{s+1}\left(\{q\}_s+\frac{a_4}{a_3}\{\dot{q}\}_s+\frac{a_5}{a_3}\{\ddot{q}\}_s\right)$

Determine $\{\ddot{q}\}_{t=0}$ is given by

$$\left\langle\{\ddot{q}\}\right|_{t=0}=[M]^{-1}\left\{\{F\}-[K]\left\langle\{q\}\right|_{t=0}\right\} \tag{41}$$

4. Result and discussion

A dynamic bending analysis of SWCNTRC plate subjected to hygro-thermo-mechanical loading for FE code in MATLAB-13a has been developed. In the present HSDT model a nine noded isoperimetric element with 63 DOF per element as shown in Fig. 2. Nine nodes per element are used to discretizing the SWCNTRC plate with 4X4 meshing. We first need to determine the effective material properties of SWCNTRC. Poly (methyl methacrylate) PMMA is selected for matrix and material properties of which are taken from (Wang *et al.* 2012)

$\rho^m=1150\,kg/m^3$, $\chi^m=0.33$, $v^m=0.34$,

$\alpha^m=45\left(1+0.0005\Delta T\right)\times10^{-6}/K$,

$T_{CO}=216^oC$

$E^m=\left(3.52-0.0034T\right)GPa$.

The (10,10) SWCNTs are selected as reinforcements (Wang *et al.* 2012) and the material properties of which at 300,500 and 700K are obtained from molecular dynamic simulation and are listed Table 1.

The effect of the time step on the accuracy of the solution was investigated by using parametric study under hygro-thermo-mechanical step loading. The non-dimensional central transvers deflection, $w_0=\bar{w}\left(\frac{E_2h^3}{q_0a^4}\right)10^2$, at selective time for time step is 0 to 0.2 seconds. Over all analysis $\delta t=0.02$ is used. $\gamma=0.5$ and $\alpha=0.5$ so that–constant average acceleration (stable) condition. The boundary condition can be written as

a) All edges are simply supported (SSSS):

$u=v=w=\psi_y=\theta_y=0$ at x=0 and a. ;

$u=v=w=\psi_x=\theta_x=0$ at y=0 and b.

b) All edges are clamped (CCCC):

$u=v=w=\psi_x=\psi_y=\theta_x=\theta_y=0$ at x=0, a and y=0, b

c) Two opposite edges are clamped and other two are simply supported (CSCS):

$u=v=w=\psi_x=\psi_y=\theta_x=\theta_y=0, at\ x=0\ and\ y=0$

$u=w=\psi_y=\theta_y=0\ at\ x=a$ and

$u=w=\psi_x=\theta_x=0 at\ y=b$

Where, a & b are length and width of SWCNTR composite plate respectively.

4.1 Comparison studies

The comparison study is carried out in this section. As mentioned earlier, there is no work reported on dynamic analysis of SWCNTRC plate. However, in this study to assure the validity of dynamic analysis of SWCNTRC plate based on HSDT. The forced time-domain responses of SWCNTRC plate subjected to hygro-thermo-mechanical loads are presented. The non-dimensional central deflection versus time (t) curves for a laminated square plate subjected to hygro-thermo-mechanical loading is plotted as shown in Fig. 3. The non-dimensional central deflection versus time (t) curves for a laminated square plate subjected to hygro-thermo-mechanical load are plotted and compared in Fig. 4.

With their material properties of plate is given (Wang *et al.* 2016) for validation purpose, E=71.238Gpa, $v=0.33$; The alumina face sheet and Ec=60MPa Gc=21MPa $v_c=0.2$ for the PVC foam core. The mass density of plate is taken to be $\rho=308.27\,kg/m^3$.

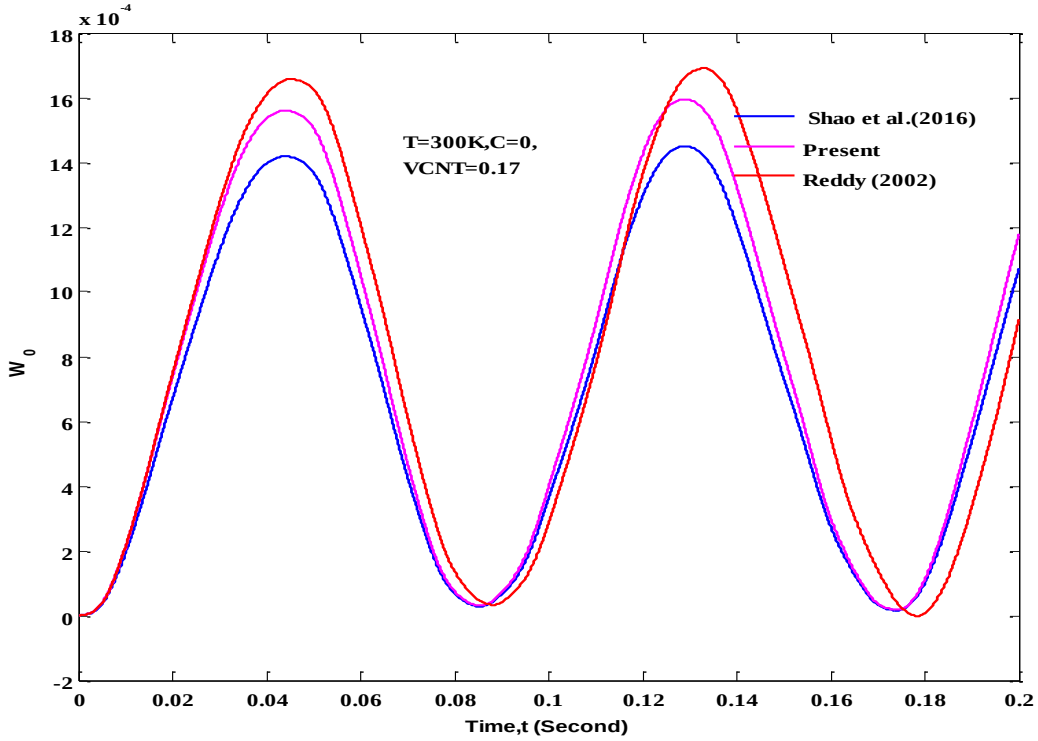

Fig. 3 Comparison of dynamic displacement response of composite plate subjected to hygro-thermo-mechanical load with (T=300K, C=0 and V_{CNT}=0.17)

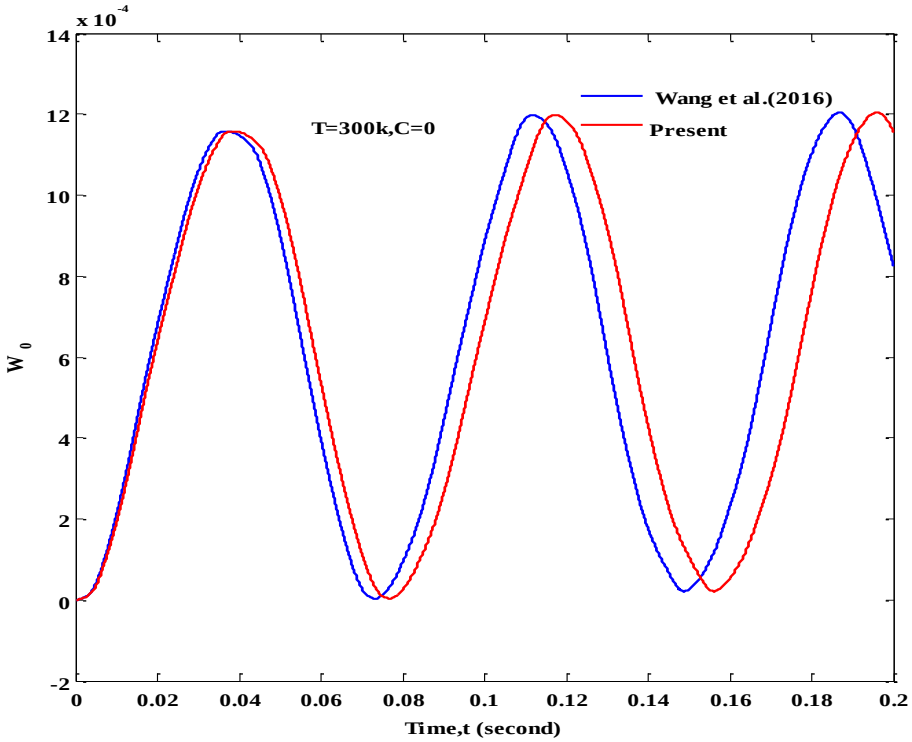

Fig. 4 Non-dimensional central transvers deflection W_0 versus time (t) for simply supported plate subjected to hygro-thermo-mechanical loading

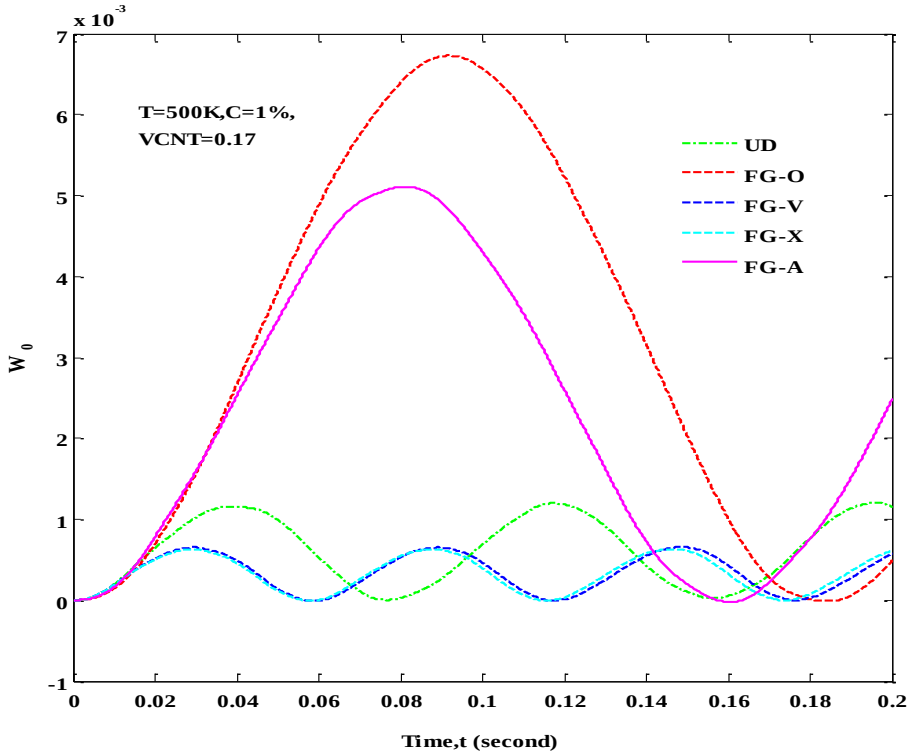

Fig. 5 The effects of functionally graded SWCNT reinforced on the dynamic displacement resonance of SWCNTRC-FG plates under hygro-thermo-mechanical loading

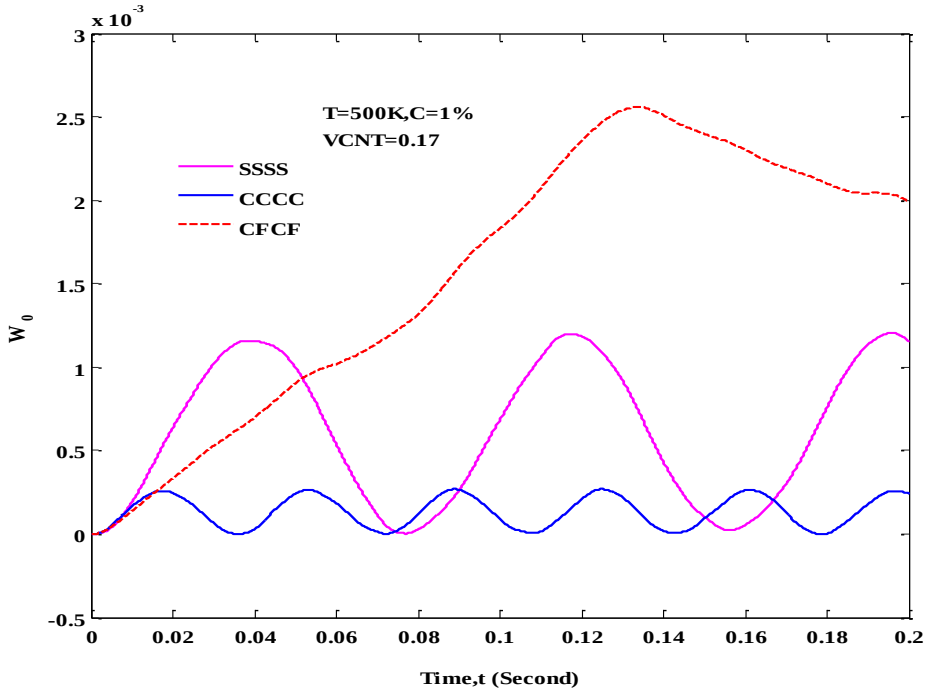

Fig. 6 The effects of boundary condition on the dynamic displacement response of SWCNTRC plates subjected to hygro-thermo-mechanical loading

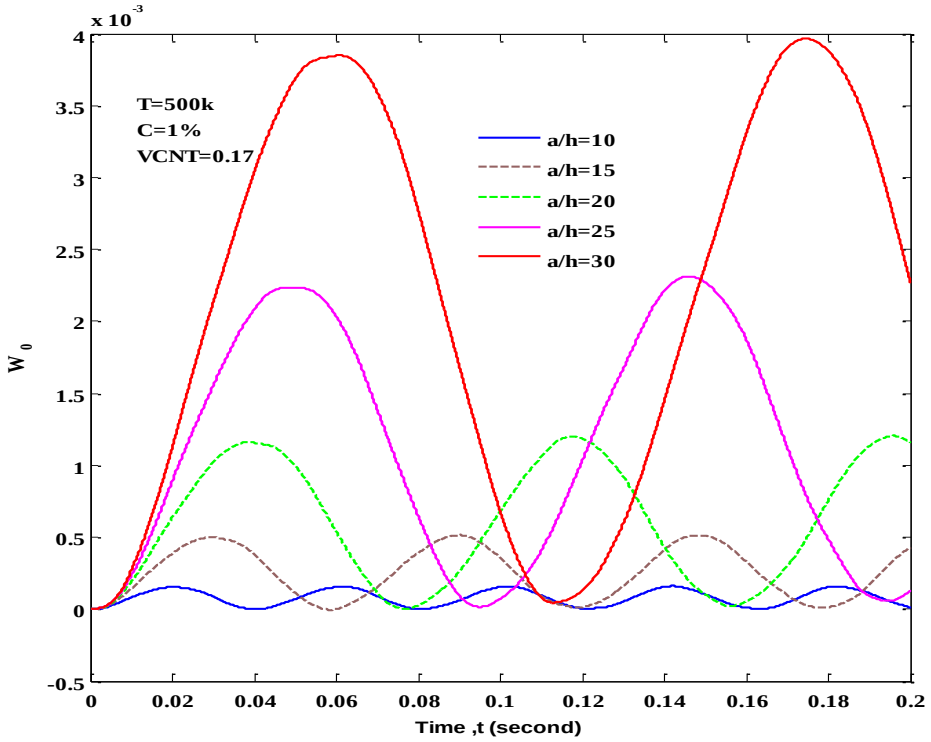

Fig. 7 The effects of width-to-thickness ratio (a/h) on the dynamic displacement response of SWCNTRC plates subjected to hygro-thermo-mechanical loading with T=500k, C=1% and V_{CNT}=0.17

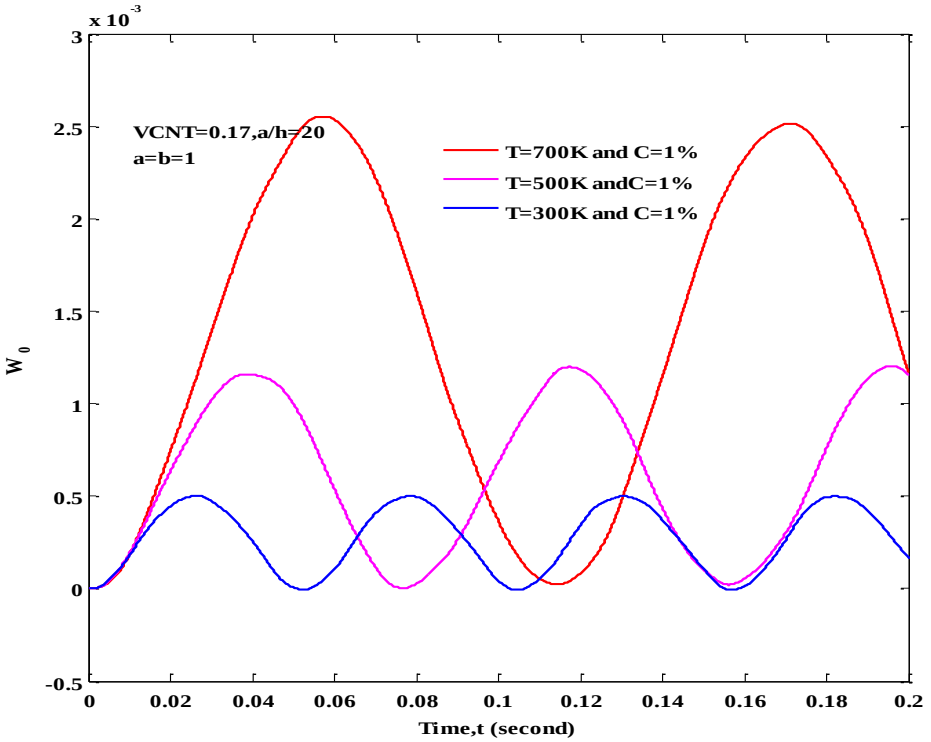

Fig. 8 The effects of different temperature on the dynamic displacement response of SWCNTRC plates under hygro-thermo-mechanical loading

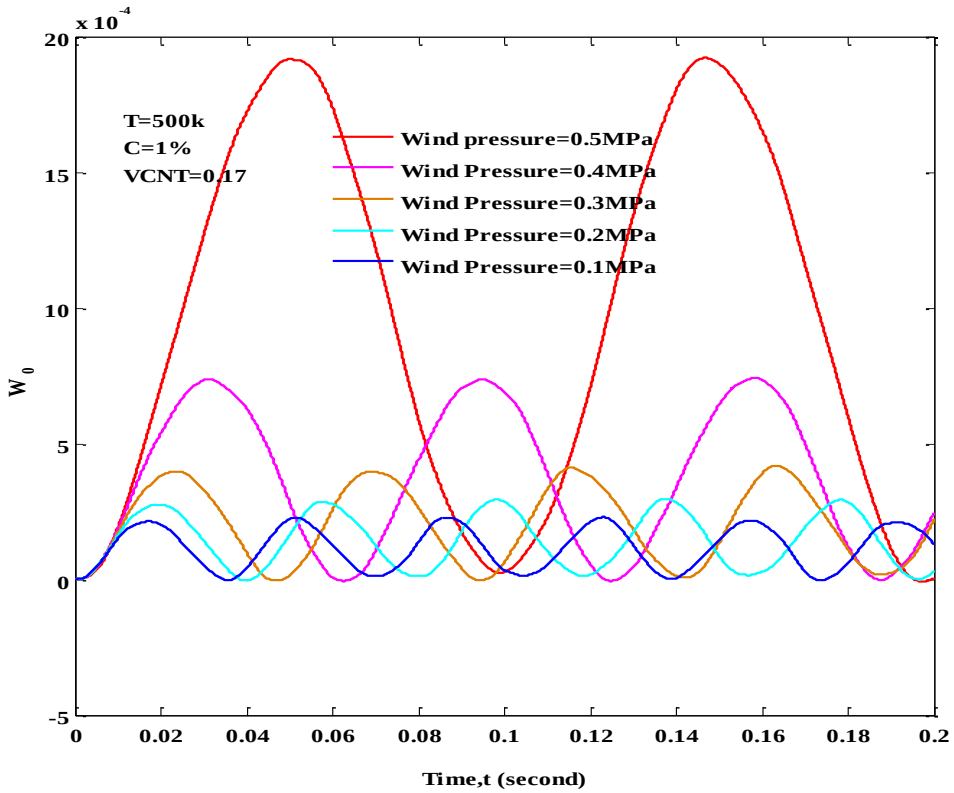

Fig. 9 The effects of different wind pressure on the dynamic displacement response of SWCNTRC plates subjected to hygro-thermo-mechanical loading with T=500k, C=1% and V_{CNT}=0.17

The Geometric properties and force data of Sandwich plate is given by 0.5 mm thick alumina face sheet and 13 mm thick PVC core and a=b=500 mm and q_0=40Pa respectively. These two comparisons show that the present results agree well with published results.

4.2 Parametric studies

Parametric studies are first carried out to examine the dynamic displacement response of FG-SWCNTRC plates subjected to hygro-thermo-mechanical loading. Five types of FG-CNTRC plates, i.e., UD, FG-V, FG-*O*, *FG-A* and FG-X, are considered. The plate geometric parameter are taken to be *a/b* = 1, *b/h* = 20, *h* = 0.358 mm and hygrothermal properties are (T=300, 500, 700K) and moisture content (C=1%) respectively. The time step for newmark integration scheme is $\delta t = 0.002$. The mechanical load considered as wind pressure to be a suddenly applied uniform load with q_0 = 0.5 MPa. Fig. 4 presents the dynamic response of five types of FG-SWCNTRC plates. The width-to-thickness ratio and volume fraction are taken to be 20 and 0.17 respectively. It can be seen that the FG-X and FG-V plates are lowest deflection while FG-O and FG-A plates are large deflection. Hence, above study only UD and FG-X plate are considered. Fig. 5 shows effects of functional graded SWCNT reinforced on the dynamic displacement resonance of FG-SWCNTRC plates under hygro-thermo-mechanical loading. It can be seen that FG-X plate is harder than that of other type of plate in hygro-thermal environment. Fig. 6 depict the effects of boundary condition on the dynamic displacement response of SWCNTRC plates subjected to hygro-thermo-mechanical loading with temperature=500k and moisture 1% and volume fraction of SWCNT=0.17. It can be seen that the curve of deflection higher for CFCF boundary condition while lower deflection in CCCC boundary condition. Hence, CCCC boundary condition is large stiffness as compared to other type of boundary condition. Fig. 7 presents effects of width-to-thickness ratio (a/h) on the dynamic displacement response of SWCNTRC plates subjected to hygro-thermo-mechanical loading with T=500k, C=1% and V_{CNT}=0.17. It can be seen that the curve of deflection higher at a/h=30.

Increase the deflection with increasing width-to-thickness ratio of SWCNTRC plate in hygro-thermal environment is found. Fig. 8 shows effects of different temperature on the dynamic displacement response of SWCNTRC plates under hygro-thermo-mechanical loading. It can be seen that non-dimensional central deflection is higher at T=700K while lower deflection at T=300K. When, increased the displacement with an increasing temperature of SWCNTRC plate. Fig. 9 shows the effects of different wind pressure on the dynamic displacement response of SWCNTRC plates subjected to hygro-thermo-mechanical loading with T=500k, C=1% and V_{CNT}=0.17. It can be seen that increased the deflection of SWCNTRC plates with increasing wind pressure.

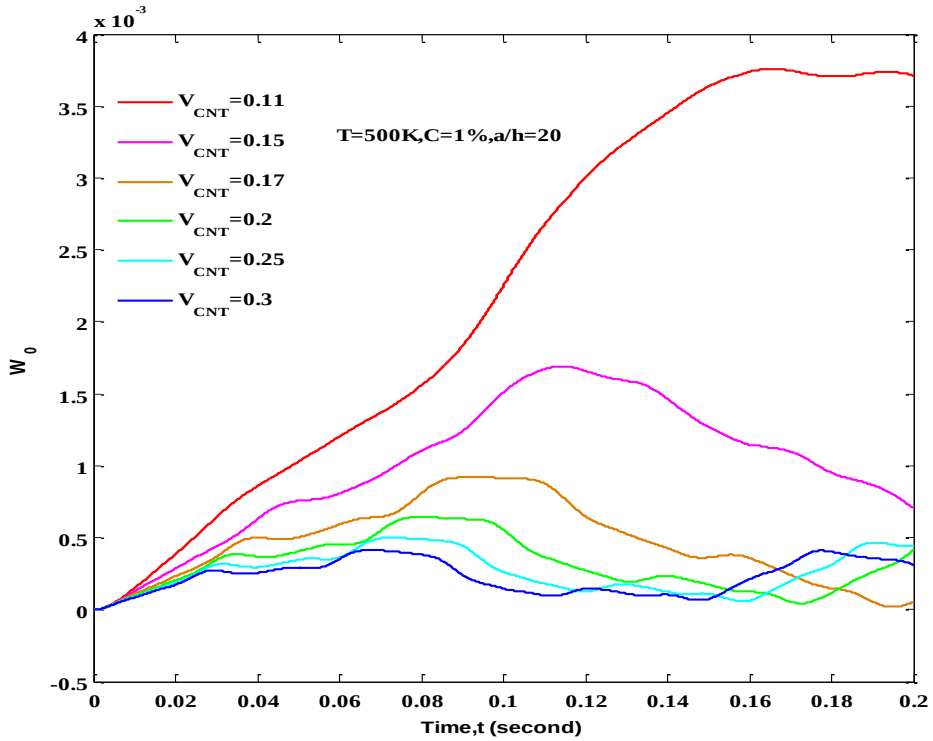

Fig. 10 The effects of different volume fraction of SWCNT on the dynamic displacement response of SWCNTRC plates under hygro-thermo-mechanical loading

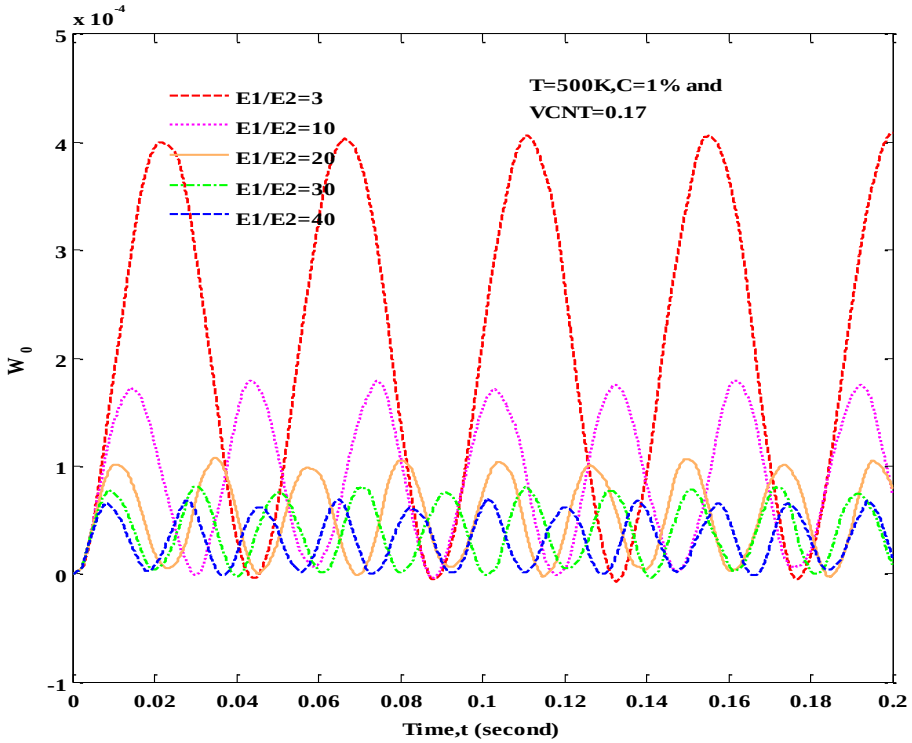

Fig. 11 The effects of E_1/E_2 ratio on the dynamic displacement response of SWCNTRC plates under hygro-thermo-mechanical loading with T=500k, C=1% and V_{CNT}=0.17

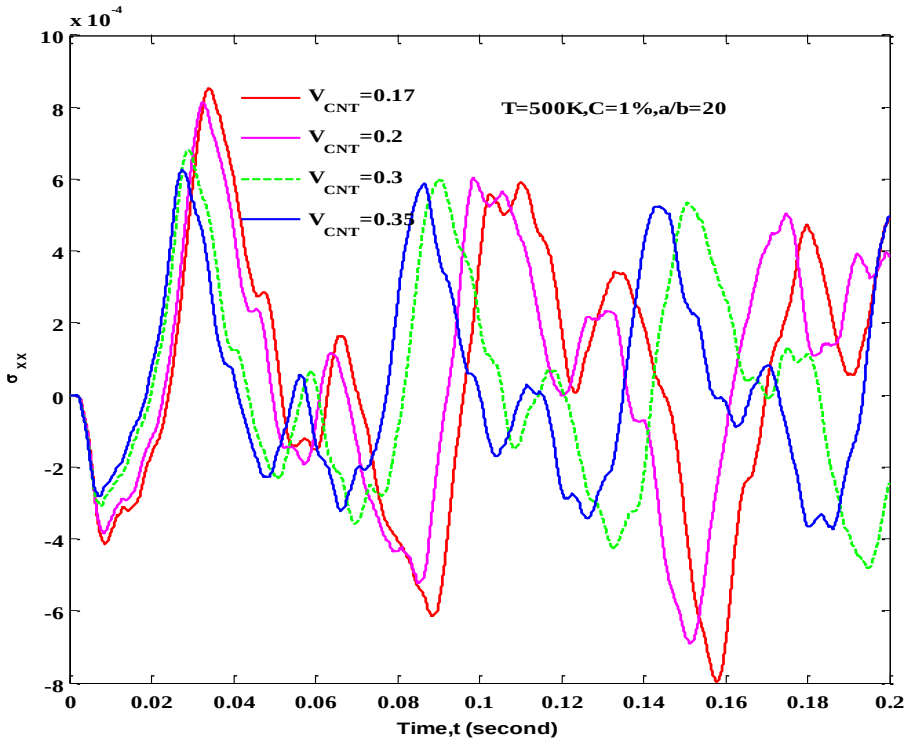

Fig. 12 Non-dimensional normal stress (σ_{xx}) versus time (t) for simply supported SWCNTRC plate subjected to hygro-thermo-mechanical loading

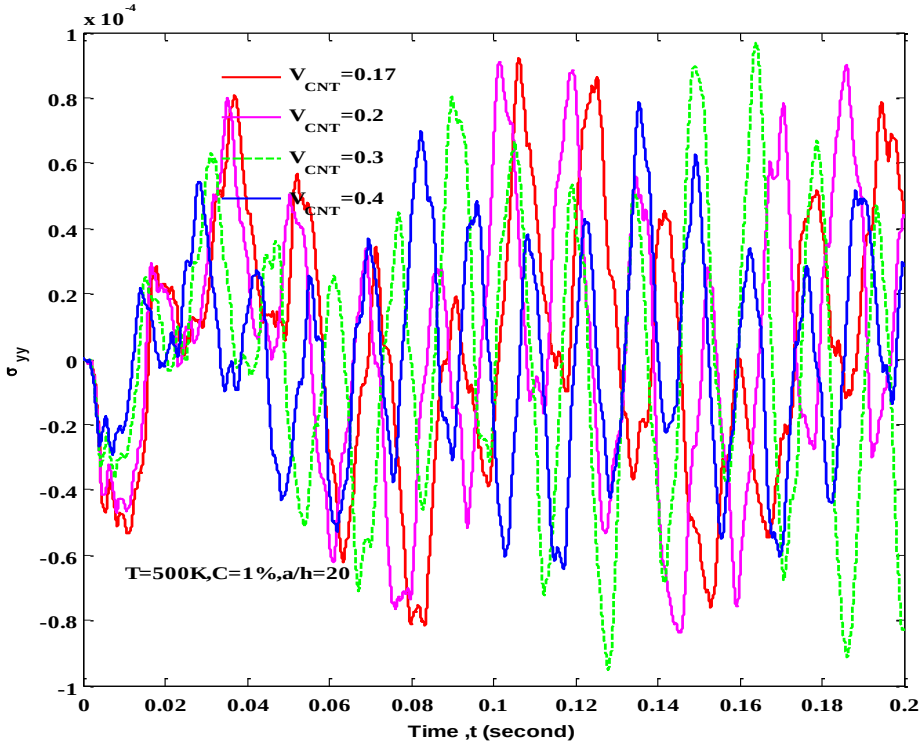

Fig. 13 Non-dimensional normal stress (σ_{yy}) versus time (t) for simply supported SWCNTRC plate subjected to hygro-thermo-mechanical loading with T=500K, C=1% and a/h=20

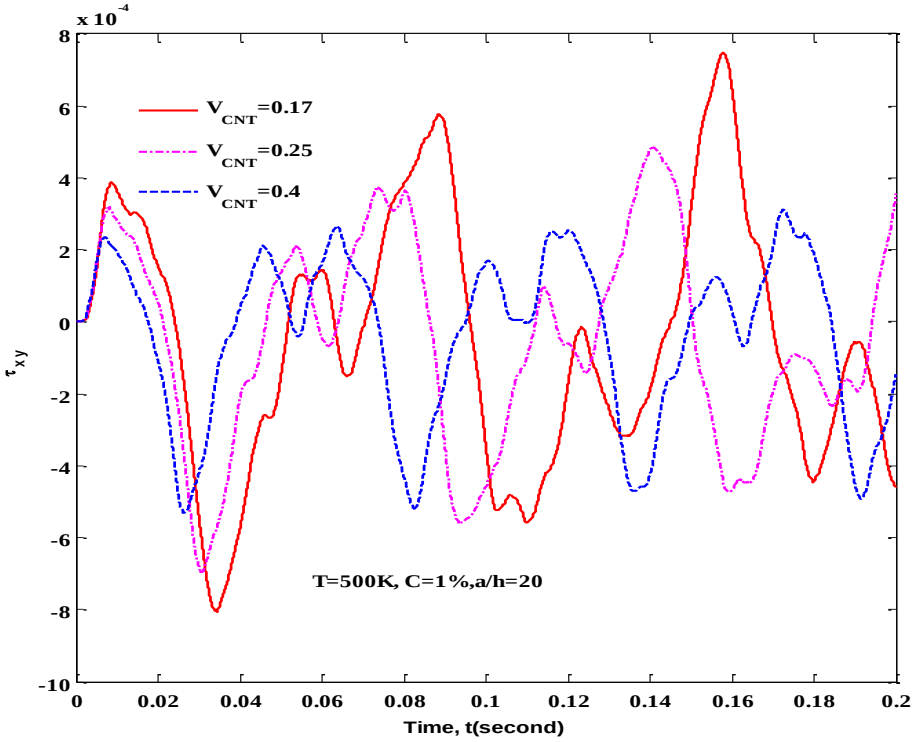

Fig. 14 Non-dimensional shear stress (τ_{xy}) versus time (t) for simply supported SWCNTRC plate subjected to hygro-thermo-mechanical loading

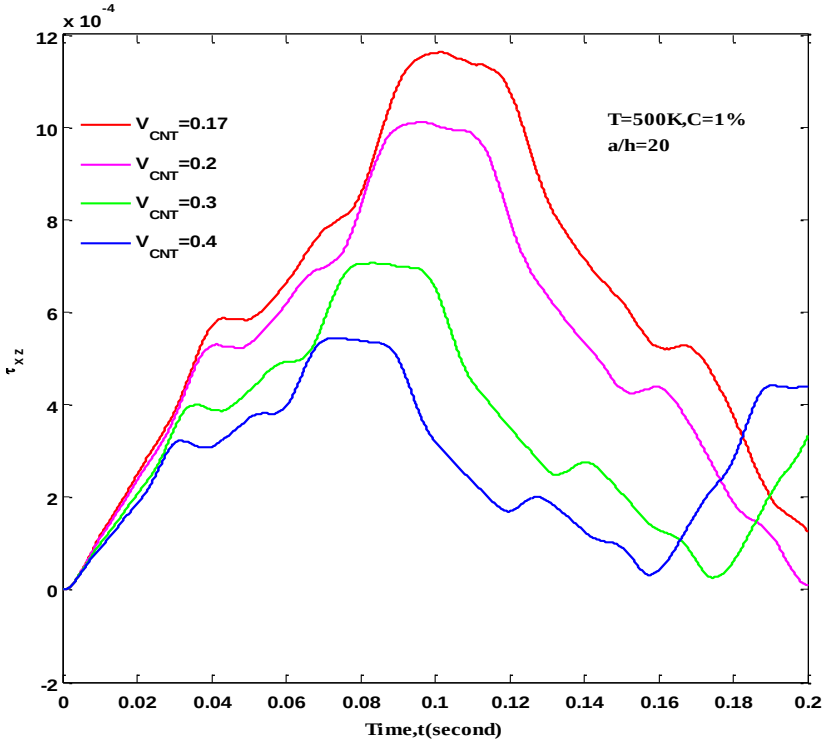

Fig. 15 Non-dimensional shear stress (τ_{xz}) versus time (t) for simply supported SWCNTRC plate subjected to hygro-thermo-mechanical loading

Fig. 10 presents the effect of volume fraction of SWCNT with CCCC boundary condition on dynamic displacement response of SWCNTRC plates subjected to hygro-thermo-mechanical loading. It can be seen that decrease the deflection of SWCNTRC plates with increasing volume fraction of SWCNT.

Fig. 11 shows the effects of E_1/E_2 ratio on the dynamic displacement response of SWCNTRC plates under hygro-thermo-mechanical loading with T=500K, C=1% and V_{CNT}=0.17. It can be seen that decrease the deflection of SWCNTRC plates with increasing E1/E2. Figs. 12-15 shows normal and shear stresses of SWCNTRC plate subjected to hygro-thermo-mechanical loading with T=500K C=1% by various volume fraction of SWCNT. The normal and shear stresses are decreased due to increasing volume fraction of SWCNT

5 Conclusions

The dynamic version of the High Order shear deformation Theory (HSDT) for single carbon nanotube reinforced composite (SWCNTRC) plate. Dynamic responses of SWCNTRC plates subjected to hygro-thermo-mechanical loading have been presented. However, for dynamic analysis, the solution is obtained in the time domain by implementing Newmark method. The mechanical load as wind pressure is considered for dynamic response of SWCNTRC plate. Two cases of in-plane boundary conditions are considered. The parametric studies have been carried out after two comparisons which demonstrated the accuracy and effectiveness of the present method. The effects of boundary conditions on dynamic bending response of the SWCNTRC plate are investigated. In each type of boundary condition the effects of carbon nanotube volume fraction and their distribution pattern, width-to-thickness ratio on many essential involved parameters of the SWCNTRC plate with functionally graded carbon nanotube reinforced composite (FG-CNTRC) are studied in detail. Finally concluded following points

- The five different grading profiles, namely, UD, FG-V, FG-X,FG-A and FG-O on the time domain response of the SWCNTRC plate, the displacement amplitude is the highest for FG-O, out of FG-A, UD, FG-X and FG-V.
- The central deflection of SWCNTRC plate is increased with increasing the hygro-thermo-mechanical load.
- The non-dimensional central displacement of SWCNTRC plate is increased with an increasing the a/h of the SWCNTRC plate subjected to hygro-thermal environment.

The central deflection decreased with increasing volume fraction of SWCNT of SWCNTRC plate subjected to hygro-thermo-mechanical loading.

References

Ahouel, M., Houari, M.S.A., Adda Bedia, E.A. and Tounsi, A. (2016), "Size-dependent mechanical behavior of functionally graded trigonometric shear deformable nanobeams including neutral surface position concept", *Steel Compos. Struct.*, **20**(5) 963-981..

Ait Amar Meziane et al (2014), "An efficient and simple refined theory for buckling and free vibration of exponentially graded sandwich plates under various boundary conditions", *J. Sandw. Struct. Mater.*, **16**(3), 293-318.

Ait Yahia, S., Ait Atmane, H., Houari, M.S.A. and Tounsi, A. (2015), "Wave propagation in functionally graded plates with porosities using various higher-order shear deformation plate theories", *Struct. Eng. Mech.*, **53**(6), 1143-1165.

Al-Basyouni, K.S., Tounsi, A. and Mahmoud, S.R. (2015), "Size dependent bending and vibration analysis of functionally graded micro beams based on modified couple stress theory and neutral surface position", *Compos. Struct.*, **125**, 621-630.

Amen, A. and Jean Pierre, M. (2006), "A layered approach to the non-linear static and dynamic analysis of rectangular reinforced concrete slabs", *J. Mech. Sci.*, **48**(3), 294-306.

Asadi, H., Bodaghi, M., Shakeri, M. and Aghdam, M.M. (2014), "Nonlinear dynamics of SMA-fiber-reinforced composite beams subjected to a primary/secondary-resonance excitation", *Acta Mech.*, **226**(2), 437-455.

Belabed, Z., Houari, M.S.A., Tounsi, A., Mahmoud, S.R. and Anwar Beg, O. (2014), "An efficient and simple higher order shear and normal deformation theory for functionally graded material (FGM) plates", *Compos.*: *Part B*, **60**, 274-283.

Beldjelili, Y., Tounsi, A. and Mahmoud, S.R. (2016), "Hygrothermo-mechanical bending of S-FGM plates resting on variable elastic foundations using a four-variable trigonometric plate theory", *Smart Struct. Syst.*, **18**(4), 755-786.

Belkorissat, I., Houari, M.S.A., Tounsi, A., Adda Bedia, E.A. and Mahmoud, S.R. (2015), "On vibration properties of functionally graded nano-plate using a new nonlocal refined four variable model", *Steel Compos. Struct.*, **18**(4), 1063-1081.

Bellifa, H., Benrahou, K.H., Hadji, L., Houari, M.S.A. and Tounsi, A. (2016), "Bending and free vibration analysis of functionally graded plates using a simple shear deformation theory and the concept the neutral surface position", *J. Braz. Soc. Mech. Sci. Eng.*, **38**(1), 265-275.

Benahmed, A., Houari, M.S.A., Benyoucef, S., Belakhdar, K. and Tounsi, A. (2017), "A novel quasi-3D hyperbolic shear deformation theory for functionally graded thick rectangular plates on elastic foundation", *Geomech. Eng.*, **12**(1), 9-34.

Benguediab, S., Tounsi, A., Zidour, M. and Semmah, A. (2014), "Chirality and scale rffects on mechanical buckling properties of zigzag double-walled carbon nanotubes", *Compos. Part B*, **57**, 21-24.

Bennoun, M., Houari, M.S.A. and Tounsi, A. (2016), "A novel five variable refined plate theory for vibration analysis of functionally graded sandwich plates", *Mech. Adv. Mater. Struct.*, **23**(4), 423-431.

Bodaghi, M., Damanpack, A.R., Aghdam, M.M. and Shakeri, M. (2013), "Active shape/stress control of shape memory alloy laminated beams", *Compos.*: *Part B*, **56**, 889-899.

Bouafia, K., Kaci, A., Houri, M.S.A., Benzair, A. and Tounsi, A. (2017), "A nonlocal quasi-3D theory for bending and free flexural vibration behaviors of functionally graded nanobeams", *Smart Struct. Syst.*, **19**(2), 115-126.

Bouderba, B., Houari, M.S.A., Tounsi, A. and Mahmoud, S.R. (2016), "Thermal stability of functionally graded sandwich plates using a simple shear deformation theory", *Struct. Eng. Mech.*, **58**(3), 397-422.

Bounouara, F., Benrahou, K.H., Belkorissat, I. and Tounsi, A.

(2016), "A nonlocal zeroth-order shear deformation theory for free vibration of functionally graded nanoscale plates resting on elastic foundation", *Steel Compos. Struct.*, **20**(2), 227-249.

Bourada, F., Amara, K. and Tounsi, A. (2016), "Buckling analysis of isotropic and orthotropic plates using a novel four variable refined plate theory", *Steel Compos. Struct.*, **21**(6), 1287-1306.

Bourada, M., Kaci, A., Houari, M.S.A. and Tounsi, A. (2015), "A new simple shear and normal deformations theory for functionally graded beams", *Steel Compos. Struct.*, **18**(2), 409-423.

Bousahla, A.A., Houari, M.S.A., Tounsi, A. and Adda Bedia, E.A. (2014), "A novel higher order shear and normal deformation theory based on neutral surface position for bending analysis of advanced composite plates", *J. Comput. Meth.*, **11**(6), 1350082.

Chavan, S.G. and Lal, A. (2017), "Bending analysis of laminated SWCNT Reinforced functionally graded plate Using FEM", *Curv. Lay. Struct.*, **4**(1), 133-144.

Chen, W.Q. and Lee, K.Y. (2005), "State-space approach for statics and dynamics of angle-ply laminated cylindrical panels in cylindrical bending", *J. Mech. Sci.*, **47**, 374-387.

Chikh, A., Tounsi, A., Hebali, H. and Mahmoud, S.R. (2017), "Thermal buckling analysis of cross-ply laminated plates using a simplified HSDT", *Smart Struct. Syst.*, **19**(3), 289-297.

Shao, D., Hu, F., Wang, Q., Fuzhen, P. and Hu, S. (2016), "Transient response analysis of cross-ply composite laminated rectangular plates with general boundary restraints by the method of reverberation ray matrix", *Compos. Struct.*, **152**, 168-182.

Ebrahimi, F. and Habibi, S. (2017), "Nonlinear eccentric low-velocity impact response of polymer-CNT-fiber multiscale nanocomposite plate resting on elastic foundations in hygrothermal environments", *Mech. Adv. Mater. Struct.*, 1-14.

Gadade, A.M., Lal, A. and Shing, B.N. (2016), "Acurate stochastic initial and finial faluare of laminated plates subjected to hygro-thermo-mechanival loadings using puck's failure criteria", *J. Mech. Sci.*, **114**,177-206.

Girhammar, U.A., Pan Dan, H. and Gustafsson, A. (2009), "Exact dynamic analysis of composite beams with partial interaction", *J. Mech. Sci.*, **51**, 565-582.

Habib, H., Tounsi, A., Houari, M.S.A., Bessaim, A. and Bedia, E.A.A. (2014), "A new quasi-3D hyperbolic shear deformation theory for the static and free vibration analysis of functionally graded plates", *ASCE J. Eng. Mech.*, **140**, 374-383.

Hamidi, A., Houari, M.S.A., Mahmoud, S.R. and Tounsi, A. (2015), "A sinusoidal plate theory with 5-unknowns and stretching effect for thermo-mechanical bending of functionally graded sandwich plates", *Steel Compos. Struct.*, **18**(1), 235-253.

Houari, M.S.A., Tounsi, A., Bessaim, A. and Mahmoud, S.R. (2016), "A new simple three-unknown sinusoidal shear deformation theory for functionally graded plates", *Steel Compos. Struct.*, **22**(2), 257-276.

Kamarian, S., Shakeri, M., Yas, M.H., Bodaghi, M. and Pourasghar, A. (2017), "Free vibration analysis of functionally graded nanocomposite sandwich beams resting on pasternak foundation by considering the agglomeration effect of CNTs", *J. Sandw. Struct. Mater.*, 1-34.

Kamarian, S., Bodaghi, M., Pourasghar, A. and Talebi, S. (2016), "Vibrational behavior of non-uniform piezoelectric sandwich beams made of CNT-reinforced polymer nanocomposite by considering the agglomeration effect of CNTs", *Polym. Compos.*, 1-10.

Khatibinia, M., Feizbakhsh, A., Mohseni, E. and Ranjbar, M.M. (2016), "Modeling mechanical strength of self-compacting mortar containing nanoparticles using wavelet-based support vector machine", *Comput. Concrete*, **18**(6), 1065-1082.

Larbi, C.F., Kaci, A., Houari, M.S.A., Tounsi, A., Anwar, B.O. and Mahmoud, S.R. (2015), "Bending and buckling analyses of functionally graded material (FGM) size-dependent nanoscale beams including the thickness stretching effect", *Steel Compos. Struct.*, **18**(2), 425-442.

Lei, Z.X., Zhang, L.W. and Liew, K.M. (2015), "Elastodynamic analysis of carbon nanotube-reinforced functionally graded plates", *J. Mech. Sci.*, **99**, 208-217.

Liew, K.M., He, X.Q., Tan, M.J. and Lim, H.K. (2004), "Dynamic analysis of laminated composite plates with piezoelectric sensor/actuator patches using the FSDT mesh-free method", *J. Mech. Sci.*, **46**, 411-431.

Liew, K.M., Lee, Y.Y., Ng, T.Y. and Zhao, X. (2007), "Dynamic stability analysis of composite laminated cylindrical panels via the mesh-free kp-Ritz method", *J. Mech. Sci.*, **49**, 1156-1165.

Mahi, A., Adda Bedia, E.A. and Tounsi, A. (2015), "A new hyperbolic shear deformation theory for bending and free vibration analysis of isotropic, functionally graded, sandwich and laminated composite plates", *Appl. Math. Model.*, **39**, 2489-2508.

Nan, Li, Mabrouk, B.T., Zoheir, A. and Kamel, K. (2016), "A dynamic analysis approach for identifying the elastic properties of unstitched and stitched composite plates", *Compos. Struct.*, **152**, 959-968.

Patel, S.N., Datta, P.K. and Sheikh, A.H. (2007), "Dynamic instability analysis of stiffened shell panels subjected to partial edge loading along the edges", *J. Mech. Sci.*, **49**, 1309-1324.

Kumar, R., Ramachandra, L.S. and Banerjee, B. (2015), "Dynamic instability of damped composite skew plates under non-uniform in-plane periodic loading", *J. Mech. Sci.*, **103**, 74-88.

Ravi, K.L., Datta, P.K. and Prabhakara, D.L. (2003), "Dynamic instability characteristics of laminated composite plates subjected to partial follower edge load with damping", *J. Mech. Sci.*, **45**, 1429-1448.

Reddy, J.N. (2003), *Mechanics of Laminated Composite Plates and Shells: Theory and Analysis*, CRC Press.

Reddy, J.N. (1982), "On the solution to force motions of rectangular composite plates", *J. Appl. Mech.*, **49**, 403-408.

Salami, S.J. (2016), *Dynamic Extended high Order Sandwich Panel Theory for Transient Response of Sandwich Beams with Carbon Nanotube Reinforced Face Sheets*, Aerospace Science and Technology.

Santiuste C., Sanchez-Saez, S., Barbero, E. (2008), "Dynamic analysis of bending-torsion coupled composite beams using the flexibility influence function method", *J. Mech. Sci.*, **50**, 1611-1618.

Shariq, M., Abbas, H. and Prasad, J. (2017), "Effect of GGBFS on time dependant deflection of Rc beam", *Comput. Concrete*, **19**(1), 51-58.

Tagrara, S.H., Benachour, A., Bachir Bouiadjra, M. and Tounsi, A. (2015), "On bending, buckling and vibration responses of functionally graded carbon nanotube-reinforced composite beams", *Steel Compos. Struct.*, **19**(5), 1259-1277.

Tounsi, A., Houari, M.S.A. and Bessaim, A. (2016), "A new 3-unknowns non-polynomial plate theory for buckling and vibration of functionally graded sandwich plate", *Struct. Eng. Mech.*, **60**(4), 547-565.

Tounsi, A., Houari, M.S.A., Benyoucef, S. and Adda Bedia, E.A. (2013), "A refined trigonometric shear deformation theory for thermoelastic bending of functionally graded sandwich plates", *Aerosp. Sci. Technol.*, **24**, 209-220.

Wang, Z.X. and Shen, H.S. (2012), "Nonlinear vibration and bending of sandwich plates with nanobube reinforced composite face sheets", *Compos. Part-B*, **43**, 411-421.

Zemri, A., Houari, M.S.A., Bousahla, A.A. and Tounsi, A. (2015), "A mechanical response of functionally graded nanoscale beam: An assessment of a refined nonlocal shear deformation theory beam theory", *Struct. Eng. Mech.*, **54**(4), 693-710.

Zhang, W., Lu, S.F. and Yang, X.D. (2013), "Analysis on nonlinear

dynamics of a deploying composite laminated cantilever plate", *Nonlinear Dynam*., **76**, 69-93.

Zhen, X.W. and Shen, H.S. (2012), "Nonlinear dynamic response of nanotube-reinforced composite plates resting on elastic foundations in thermal environments", *Nonlinear Dynam*., **70**(1), 735-754.

Zidi, M., Tounsi, A., Houari, M.S.A. and Bég, O.A. (2014), "Bending analysis of FGM plates under hygro-thermo-mechanical loading using a four variable refined plate theory", *Aerosp. Sci. Technol*., **34**, 24-34.

HK